

Fucoxanthin ameliorates oxidative injury and inflammation of human bronchial epithelial cells induced by cigarette smoke extract via the PPAR γ /NF- κ B signaling pathway

SHAOLEI CHEN¹, LIN ZHU¹ and JUN LI²

¹Department of Nursing, Shandong College of Traditional Chinese Medicine, Yantai, Shandong 264199; ²Department of General Medicine, The Third Affiliated Hospital of Nantong University, Nantong, Jiangsu 226000, P.R. China

Received June 8, 2022; Accepted August 12, 2022

DOI: 10.3892/etm.2022.11768

Abstract. Chronic obstructive pulmonary disease (COPD) is a prevalent and long-term airway disease. It has been reported that fucoxanthin (FX) exhibits anti-inflammatory and antioxidant effects. However, the underlying mechanism of FX in COPD remains unknown. Therefore, to investigate the effect of FX on COPD, BEAS-2B cells were treated with cigarette smoke extract (CSE). The viability of BEAS-2B cells treated with increasing doses of FX was assessed by Cell Counting Kit-8. Lactate dehydrogenase (LDH) levels were measured using a corresponding kit. In addition, ELISA was carried out to detect the content of TNF- α , IL-1 β and IL-6. Additionally, a TUNEL assay and western blot analysis were performed to assess the cell apoptosis rate. Furthermore, 2',7'-dichlorodihydrofluorescein diacetate was used to measure reactive oxygen species levels, while the contents of oxidative stress-associated indexes were determined using the corresponding kits. Bioinformatics analysis using the search tool for interactions of chemicals database predicted that peroxisome proliferator-activated receptor γ (PPAR γ) may be a target of FX. The binding capacity of FTX with PPAR γ was confirmed by molecular docking. The protein expression levels of the PPAR γ /NF- κ B signaling-associated factors were detected by western blot analysis. Finally, the regulatory mechanism of FX in COPD was revealed following cell treatment with the PPAR γ inhibitor, T0070907. The results demonstrated that FX enhanced CSE-induced BEAS-2B cell viability and attenuated CSE-induced BEAS-2B cell inflammation and oxidative damage, possibly via triggering PPAR γ /NF- κ B signaling. Pre-treatment of BEAS-2B cells with the PPAR γ

inhibitor, T0070907, could reverse the protective effects of FX on CSE-induced BEAS-2B cells. Overall, the present study suggested that FX could ameliorate oxidative damage as well as inflammation in CSE-treated human bronchial epithelial in patients with COPD via modulating the PPAR γ /NF- κ B signaling pathway.

Introduction

As a prevalent disease, chronic obstructive pulmonary disease (COPD) is characterized by incessant respiratory disorders as well as airflow restriction, commonly associated with airway and alveolar abnormalities (1). Dyspnea, cough and phlegm are the most frequent clinical manifestations of COPD, which usually results from constant exposure to detrimental particles or gases (2). In the majority of patients, COPD is often accompanied by other chronic diseases, which can significantly increase the incidence and mortality rate, seriously threatening human public health (3). It is widely accepted that COPD is closely associated with the abnormal reaction of airways and lung tissue to harmful gases, such as cigarette smoke or toxic particles (4). Chronic exposure to cigarette smoke often results in COPD and it has been reported that >50% of smokers eventually develop the disease (5). Therefore, smoking cessation either at home or in a hospital setting is of significant importance for preventing the development of COPD.

As one of the most naturally occurring carotenoids, fucoxanthin (FX), chiefly found in sea zones (brown algae and microalgae (diatoms)), serves a critical role in alga photosynthesis (6). It has been reported that FX has several biological properties, since it can protect against oxidative stress, tumors, bacteria, viruses, obesity and neuron injury, with minimal toxicity and side effects (7). At present, FX can be used as a weight loss health care product (8). Clinically, as a drug, FX can be used in the treatment of skin cancer, colon cancer, prostate cancer, liver cancer and other cancers (9). A previous study showed that FX promoted lipopolysaccharide (LPS)-induced acute lung injury (ALI) via inhibiting Toll-like receptor 4/major myeloid differentiation response gene 88 signaling (10). FX was also demonstrated to inhibit fibrogenesis to alleviate bleomycin-induced pulmonary fibrosis (11). Another study in asthmatic mice revealed that FX improved

Correspondence to: Dr Jun Li, Department of General Medicine The Third Affiliated Hospital of Nantong University, 60 Qingnian Middle Road, Nantong, Jiangsu 226000, P.R. China
E-mail: lijun202828@163.com

Key words: fucoxanthin, chronic obstructive pulmonary disease, human bronchial epithelial cells, cigarette smoke, PPAR γ /NF- κ B signaling

oxidative stress and airway inflammation in tracheal epithelial cells (12). Additionally, the antitumor activity of FX has been previously reported in lung cancer (13). However, the effects of FX on COPD have not been previously investigated.

A previous study demonstrated that rosiglitazone inhibited the polarization of M1 macrophages via triggering peroxisome proliferator-activated receptor γ (PPAR γ) and retinoid X receptor- α , thereby improving cigarette smoke-induced airway inflammation (14). Additionally, another study revealed that erythromycin exhibited suppressive effects on cigarette smoke-induced inflammation via triggering the PPAR γ /NF- κ B signaling pathway in macrophages (15). It was therefore hypothesized that PPAR γ may be a promising target in terms of pathophysiology and pharmacology for the improvement of COPD. PPAR γ activation possibly results in NF- κ B-dependent, CSE-induced and chemokine-modulated inflammatory responses (16). Bioinformatics analysis using the search tool for interactions of chemicals (STITCH) database predicted that PPAR γ could be a target of FX. In addition, it has been shown that FX regulates the expression of PPAR γ in 3T3-L1 cells and inhibits the uptake of glucose and mature adipocytes (17). Moreover, FX was revealed to inhibit proinflammatory cytokines by regulating NF- κ B and NLRP3 inflammasome activation (18). Thus, it was hypothesized that FX may regulate COPD via targeting the PPAR γ /NF- κ B signaling pathway.

Therefore, the present study aimed to investigate the role of FX in oxidative injury and inflammation in cigarette smoke-induced human bronchial epithelial cells of patients with COPD, as well as its underlying mechanism.

Materials and methods

Preparation of aqueous cigarette smoke extract (CSE). Firstly, three cigarettes from commercial Da Qianmen cigarettes (containing 2.5 mg of nicotine and 12 mg of tar per cigarette) were burned and the smoke was then collected in a container supplemented with 10 ml PBS using a vacuum pump. The pH of 100% CSE solution was adjusted to 7.4, followed by filtering through a 0.22- μ m sterile filter. Prior to use, the well-prepared 100% CSE was diluted in RPMI 1640 medium (Gibco; Thermo Fisher Scientific, Inc.) supplemented without FBS (19). Prior to treatment with FX, GSE-exposed cells were co-treated with 10 μ M PPAR γ inhibitor, T0070907 (Beijing BioLab Technology Co., Ltd.).

Cell culture. Human bronchial BEAS-2B cells (cat. no. BS-C1281173; Shanghai Binsui Biotechnology Co., Ltd.) were cultured in DMEM with 10% FBS (both from Gibco; Thermo Fisher Scientific, Inc.). BEAS-2B cells were cultured in medium supplemented with 1, 2 or 5% CSE for 24 h. Additionally, BEAS-2B cells were pre-treated with 5, 10, 20 and 40 μ M FX followed by treatment with 5% CSE (10). FX concentrations of 0, 5, 10, 20 and 40 μ M were used at first, and Cell Counting Kit-8 (CCK8) was used to detect cell viability. It was determined that a concentration of 40 μ M FX damaged the cells, thus concentrations of 0, 5, 10 and 20 μ M FX were selected for the experiments.

CCK-8 assay. Cells were seeded into 96-well culture plates at a density of 1×10^4 cells/well and were then treated as

mentioned. Subsequently, the cells were incubated with CCK-8 solution (Millipore Sigma) at 37°C for 3 h and the absorbance at 450 nm was decided using a microplate reader (Thermo Fisher Scientific, Inc.).

ELISA. The levels of tumor necrosis factor (TNF)- α (cat. no. H052-1), interleukin (IL)-1 β (cat. no. H002) and IL-6 (cat. no. (H007-1-1) in culture supernatants were measured using the corresponding ELISA kits. Briefly, 100 μ l cell supernatant was supplemented into each well and ELISA was carried out according to the manufacturer's instructions. Additionally, a lactate dehydrogenase (LDH; cat. no. A020-2-2) assay was used to detect LDH levels according to the manufacturer's instructions. All kits were purchased from Nanjing Jiancheng Bioengineering Institute.

TUNEL assay. BEAS-2B cells (2×10^4 cells/well) were seeded into 6-well plates and were then treated as mentioned. Subsequently, the cells were fixed with 4% paraformaldehyde at 37°C for 15 min followed by the cultivation with TUNEL solution for 1 h at 37°C. The cells were then stained with 3,3-diaminobenzidine (Sigma-Aldrich; Merck KGaA) for 10 min at room temperature according to the manufacturer's protocol. Cell nuclei were stained with 0.1 μ g/ml DAPI for 5 min at room temperature and nuclear DNA fragmentation was assessed using the DeadEnd™ Fluorometric TUNEL system (Promega Corporation). Finally, the cells were observed in five randomly selected fields under an Olympus IX71 fluorescence microscope (Olympus Corporation). TUNEL-positive cells and total cells were analyzed using ImageJ 1.8.0 software (National Institutes of Health).

Western blot analysis. Total proteins were extracted from BEAS-2B cells following treatment with RIPA lysis buffer (Shanghai Absin Biotechnology Co., Ltd.) on ice. The cells were centrifuged at 16,000 \times g for 10 min at 4°C, and the supernatant was collected for western blotting. A bicinchoninic acid protein assay kit (Thermo Fisher Scientific, Inc.) was used to detect the protein concentrations. Subsequently, protein extracts (30 μ g) were separated by 10% SDS-PAGE and were then transferred onto PVDF membranes (Sigma-Aldrich; Merck KGaA). Following the block with 5% non-fat milk for 60 min at room temperature, PVDF membranes were incubated with primary antibodies Bcl-2 (1:1,000; product code ab32124), Bax (1:1,000; product code ab32503), PPAR γ (1:1,000; product code ab272718), phosphorylated (p)-NF- κ B p65 (1:1,000; product code ab32536), NF- κ B p65 (1:1,000; product code ab207297) or GAPDH (1:1,000; product code ab9485) at 4°C overnight. Subsequently, the membranes were cultivated with goat anti-rabbit IgG H&L (HRP) preadsorbed antibody (1:5,000; product code ab7090; all from Abcam) at room temperature for 1 h. An ECL system (Beyotime Institute of Biotechnology) was used to develop the membranes and blots were analyzed using ImageJ 1.8.0 (National Institutes of Health).

Reactive oxygen species (ROS) detection. Briefly, to measure ROS levels, cells (1×10^4 cells/well) seeded into a 96-well plate were treated with 2,7-dichlorodi-hydrofluorescein diacetate (DCFH-DA; Beyotime Institute of Biotechnology) solution

(dilution, 1:1,000) at a concentration of 2 μM at 37°C for 20 min. ROS content was assessed by measuring the fluorescence intensity of each well at a wavelength of 488 and 525 nm, separately, using a microplate reader. The control group served as the baseline absorbance value to calculate the average fluorescence intensity of each group.

Detection of malondialdehyde (MDA), superoxide dismutase (SOD) and glutathione peroxidase (GSH-Px). The activities of SOD (cat. no. A001-3-1; WST-1 method), MDA (cat. no. A003-1-1; colorimetric method) and GSH-Px (cat. no. A005-1-2; colorimetric method) were assessed using the corresponding kits according to the manufacturer's protocol (Nanjing Jiancheng Bioengineering Institute) by measuring the absorbance at 450, 532 and 412 nm, respectively, with a microplate reader.

Molecular docking. ChemDraw software 21 (ChemDraw; PerkinElmer, Inc.) was used to visualize the structure of FX, which was subsequently hydrogenated using OpenBabel (v2.2.1) software and converted into a mol2 format file (20). The structure of PPAR γ was downloaded from the RCSB Protein Data Bank (PDB) webpage (<https://www.rcsb.org/>). The removal of surplus water molecules, the deletion of irrelevant small ligands originally carried and protein structure analysis were performed by opening the PDB file in PyMOL (v2.2.0) software (21). Since the predicted protein structure carried a ligand, this ligand was removed and the original ligand position was considered as the docking site. Following analysis in AutoDock (v4.2), the specific docking energy values were displayed (22). The results were analyzed using Protein-Ligand Interaction Profiler (<https://plip-tool.biotec.tu-dresden.de/plip-web>) database.

Reverse transcription-quantitative polymerase chain reaction (RT-qPCR). The total RNA that was isolated with a RNeasy Mini Kit (Qiagen China Co., Ltd) was then reversely transcribed into cDNA using M-MLV RTase and random primer (GeneCopoeia, Inc.). qPCR was performed on an ABI PRISM 7900HT (Applied Biosystems; Life Technologies; Thermo Fisher Scientific, Inc.) using SYBR Premix Ex TaqTM (Takara Bio, Inc.) or Taqman probes (Applied Biosystems; Thermo Fisher Scientific, Inc.) according to the manufacturer's protocol. The thermocycling conditions were as follows: 95°C for 5 min, followed by 40 cycles at 94°C for 15 sec, 60°C for 20 sec and 72°C for 40 sec. Relative expression levels were calculated using 2^{- $\Delta\Delta\text{C}_q$} method (23). The primers were as follows: PPAR γ forward, 5'-CCAGAAGCCTGCATTCTGC-3' and reverse, 5'-CACGGAGCTGATCCCAAAGT-3'; GAPDH forward, 5'-AATGGGCAGCCGTTAGGAAA-3' and reverse, 5'-GCGCCCAATACGACCAAATC-3'.

Database. The search tool for interactions of chemicals (STITCH) database was used to predict the targets of FX (<http://stitch.embl.de/>).

Statistical analysis. All data were analyzed using SPSS 19.0 software (IBM Corp.). All results are expressed as the mean \pm SD. The differences between multiple groups were compared using one-way ANOVA followed by Tukey's

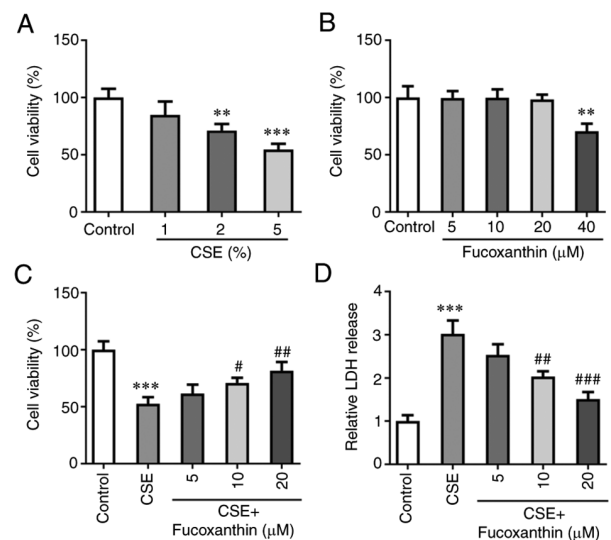


Figure 1. FX enhances CSE-induced BEAS-2B cell viability. (A) A CCK-8 assay was used to determine cell viability following CSE stimulation. ** $P < 0.01$ and *** $P < 0.001$ vs. Control. (B) A CCK-8 assay was used to determine cell viability following FX administration. ** $P < 0.01$ vs. Control. (C) A CCK-8 was used to assess cell viability of FX-treated cells exposed to CSE. *** $P < 0.001$ vs. Control; # $P < 0.05$ and ## $P < 0.01$ vs. CSE. (D) LDH release was assessed using a relative assay kit. *** $P < 0.001$ vs. Control; ## $P < 0.01$ and ### $P < 0.001$ vs. CSE. FX, fucoxanthin; CSE, cigarette smoke extract; CCK-8, Cell Counting Kit-8.

post hoc test with GraphPad Prism 5 software (GraphPad Software, Inc.). $P < 0.05$ was considered to indicate a statistically significant difference. All experiments were repeated at least three times.

Results

FX enhances CSE-induced BEAS-2B cell activity. Following exposure of BEAS-2B cells to 1, 2 or 5% CSE, cell viability was evaluated. The results of the CCK-8 assay demonstrated that cell viability of BEAS-2B cells was markedly and gradually decreased with the increasing concentrations of CSE (Fig. 1A). A concentration of 5% CSE was selected for the follow-up experiments. Subsequently, BEAS-2B cells were induced with 5, 10, 20 or 40 μM FX, and the results demonstrated that FX at concentrations of 5, 10 and 20 μM did not affect the cell viability of BEAS-2B cells, and FX at a concentration of 40 μM significantly decreased cell viability (Fig. 1B). To avoid FX-induced cell injury, concentrations of 5, 10 and 20 μM FX were selected for the subsequent experiments. Cells were then divided into the following five groups: The control group; the CSE group; the CSE + 5 μM FX group; the CSE + 10 μM FX group; and the CSE + 20 μM FX group. The results of the CCK-8 assay demonstrated that the CSE-induced decrease of cell viability was reversed with increasing concentrations of FX (Fig. 1C). Additionally, LDH levels were assessed. The results revealed that LDH production was significantly enhanced in the CSE group compared with the control group. However, compared with the CSE group, the levels of LDH were significantly reduced in the CSE + FX groups (Fig. 1D).

FX attenuates CSE-induced inflammation and oxidative damage in BEAS-2B cells. The results of ELISA demonstrated

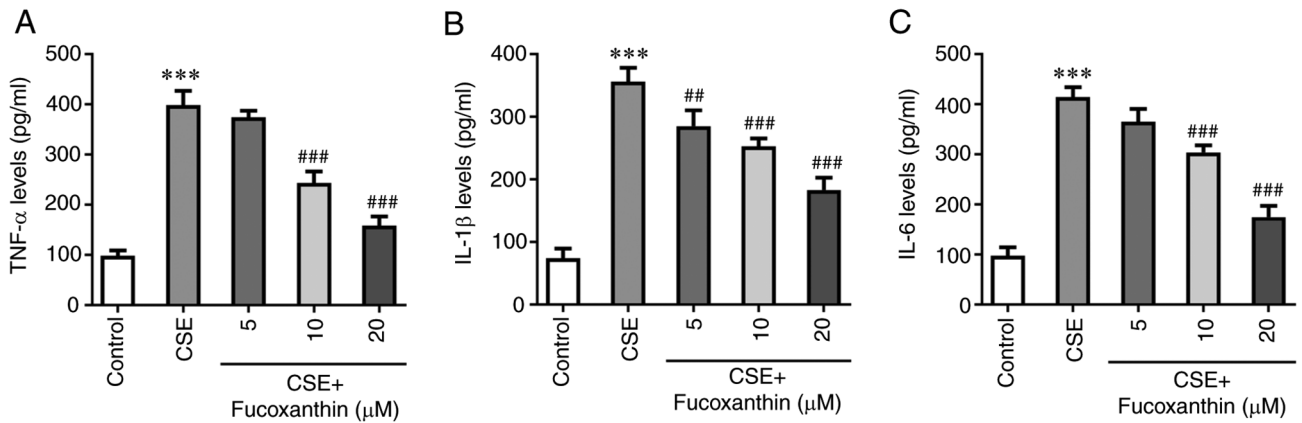


Figure 2. FX attenuates CSE-induced inflammation in BEAS-2B cells. The expression levels of (A) TNF- α , (B) IL-1 β and (C) IL-6 were examined using ELISA. *** $P < 0.001$ vs. Control; ** $P < 0.01$ and ### $P < 0.001$ vs. CSE. FX, fucoxanthin; CSE, cigarette smoke extract; TNF- α , tumor necrosis factor- α ; IL-, interleukin.

that the levels of TNF- α , IL-1 β and IL-6 were significantly increased in the CSE group compared with the control group. However, the levels of the aforementioned cytokines were decreased with increasing concentrations of FX in the CSE + FX groups compared with the CSE group (Fig. 2). TUNEL assay and western blot analysis revealed that compared with the control group, cell apoptosis was evidently enhanced in the CSE group, accompanied by Bcl-2 downregulation and Bax upregulation. Compared with the CSE group, cell apoptosis was decreased in the CSE + FX groups in a dose-dependent manner, as verified by the increased Bcl-2 expression and decreased Bax expression (Fig. 3A-C). Additionally, ROS levels were increased following cell induction with CSE compared with the control group. However, ROS production was dose-dependently reduced in CSE-induced cells after cell exposure to FX (Fig. 3D). Furthermore, MDA activity was significantly elevated, while that of SOD and GSH-Px was attenuated in the CSE-induced cells. Following cell treatment with increasing concentrations of FX, MDA activity was dose-dependently reduced, while SOD and GSH-Px activities were dose-dependently enhanced in the CSE-induced cells (Fig. 3D).

FX regulates PPAR γ /NF- κ B signaling. Bioinformatics analysis using the STITCH database predicted that PPAR γ could be a target of FX (Fig. 4A). The three-dimensional structure of PPAR γ protein was obtained from PDB database (PDB ID: 1KNU) and the Autodock (version 4.2) database was used for molecular docking (Fig. 4B). The analysis indicated that FX could regulate PPAR γ expression. In addition, western blot and RT-qPCR analyses showed that PPAR γ was downregulated and p-NF- κ B p65 was upregulated following cell treatment with CSE. However, compared with the CSE group, the expression levels of PPAR γ were gradually increased, while those of p-NF- κ B p65 were gradually reduced in the CSE + FX groups, in a dose-dependent manner (Fig. 4C and D).

Pretreatment with the PPAR γ inhibitor, T0070907, reverses the protective effects of FX on CSE-induced BEAS-2B cells. Subsequent assays were carried out using 20 μ M FX. Cells were divided into the following four groups: The control

group; the CSE group; the CSE + FX group; and the CSE + FX + T0070907 group. Cells in the CSE + FX + T0070907 group were co-treated with a PPAR γ inhibitor, namely T0070907. The results revealed that the levels of inflammatory cytokines were significantly increased in the CSE + FX + T0070907 group compared with the CSE + FX group (Fig. 5A-C). TUNEL assay and western blot analysis revealed that compared with the CSE + FX group, cell apoptosis was enhanced in the CSE + FX + T0070907 group, as indicated by Bcl-2 downregulation and Bax upregulation (Fig. 5D-G). In addition, DCFH-DA assay showed that T0070907 significantly reversed the effects of FX on ROS, MDA, SOD and GSH-Px levels in CSE-induced BEAS-2B cells (Fig. 5H-K).

Discussion

Epidemiological and genetic risk factors for COPD include long-term smoking, persistent exposure to air pollution, respiratory infections, inhalation of biofuel smoke and occupational dust (24). Among them, smoking is a pivotal risk factor, significantly contributing to the development of COPD, thus increasing the rate of impaired lung function (25,26). This could mainly be due to the harmful gases and particulate matter produced by tobacco, causing lung inflammation and oxidative stress response. In turn, lung inflammation and oxidative stress response could further lead to lung tissue injury and small airway fibrosis, eventually resulting in irreversible airflow restriction and various respiratory symptoms in individuals (27). In addition, persistent chronic inflammation induces the recurrence of vascular wall damage and repair processes, thus leading to airway remodeling, which is the primary cause of irreversible COPD progression (28). In the present study, human bronchial BEAS-2B cells were induced with CSE, thus resulting in oxidative damage and inflammatory response, simulating COPD *in vitro*. Moreover, the model of CSE-induced human bronchial epithelial cells is a recognized COPD model (14,15,19) When patients with COPD are affected by air pollutants and other inducements, the epithelial cells are stimulated to release oxidative stress-related factors SOD, GSH-Px, MDA, which lead to the accumulation of inflammation-related factors TNF- α , IL-1 β and IL-6 in the

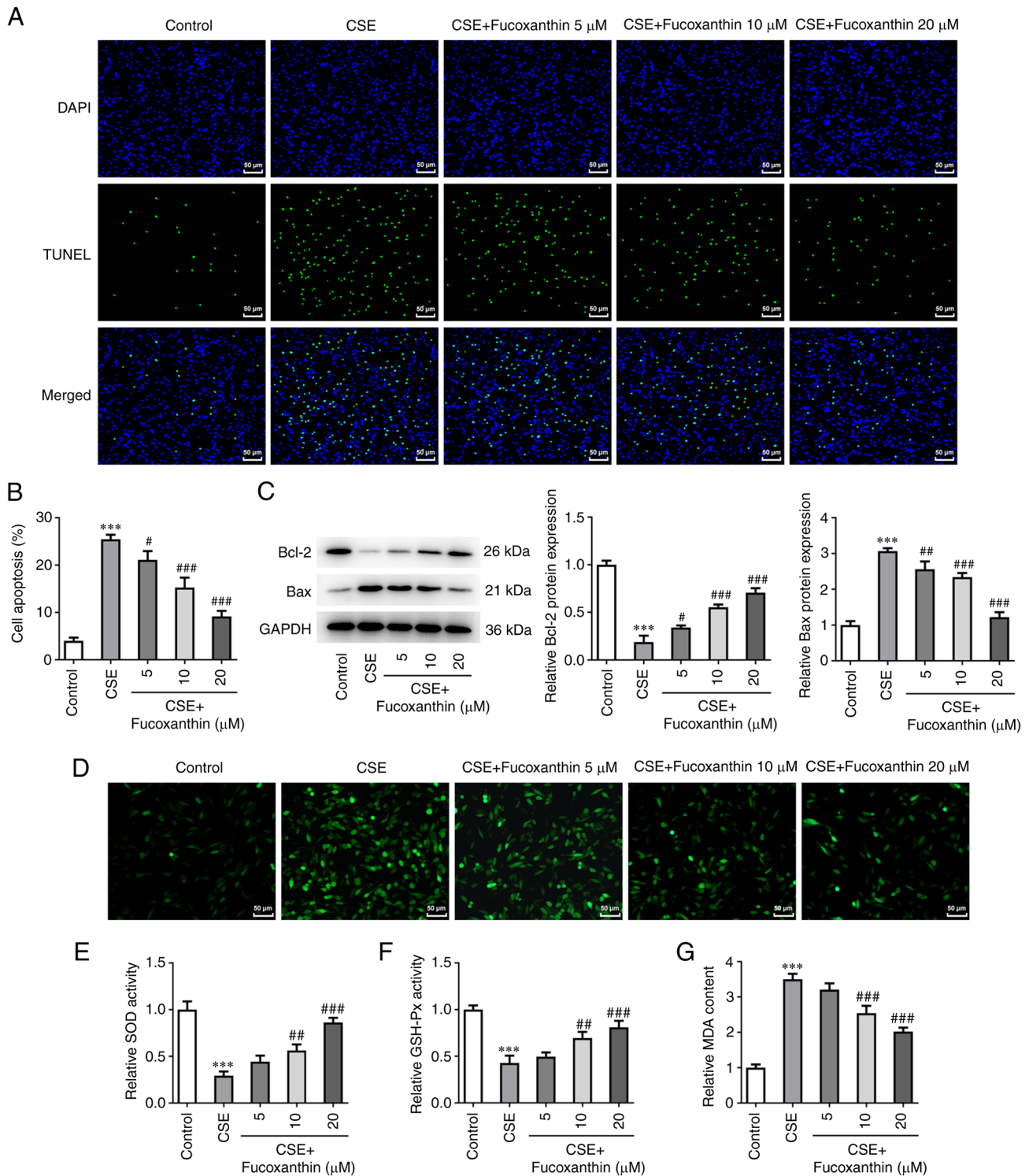


Figure 3. FX attenuates CSE-induced oxidative damage in BEAS-2B cells. (A) A TUNEL assay was used to determine the apoptotic rate of cells. (B) Statistical analysis of apoptotic cells. (C) Western blotting was used to examine the expression of Bcl-2 and Bax. (D) DCFH-DA was used to assess ROS activity. Relative kits were used to assess the levels of oxidative stress-related indicators (E) SOD, (F) GSH-Px and (G) MDA. *** $P < 0.001$ vs. Control; # $P < 0.05$, ## $P < 0.01$ and ### $P < 0.001$ vs. CSE. FX, fucoxanthin; CSE, cigarette smoke extract; ROS, reactive oxygen species; SOD, superoxide dismutase; GSH-Px, glutathione peroxidase; MDA, malondialdehyde.

airway giving rise to cell damage, and thus causing the acute exacerbation of COPD (29). Therefore, oxidative stress and inflammatory response were detected to be activated after CSE induction in the experiments of the present study.

FX, a natural carotenoid, is extensively found in various algae, marine phytoplankton and aquatic shellfish (7). This

compound can protect against inflammation, obesity, diabetes and cancer (6). It has been also reported that FX exhibits particular therapeutic effects on airway inflammatory or traumatic diseases. Therefore, a study demonstrated that FX exerted anti-inflammatory and antiapoptotic effects on lung cancer in benzo(A) pyrene-induced mice (30). In asthma, FX

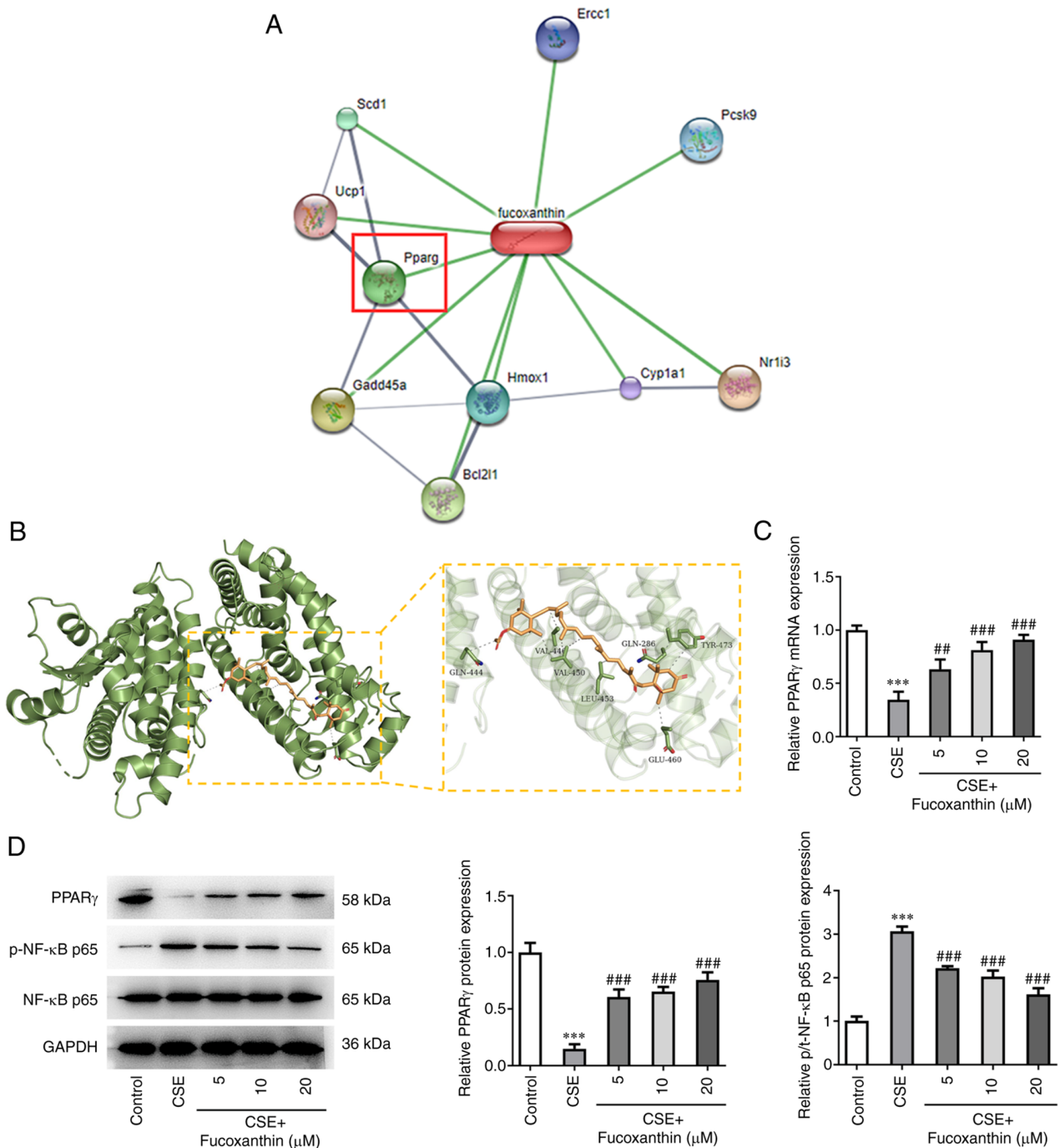


Figure 4. FX regulates PPAR γ /NF- κ B signaling. (A) STITCH predicted that PPAR γ (PPAR γ) may be one of the targets of FX. (B) Molecular docking. (C) RT-qPCR was used to detect the mRNA expression of PPAR γ . (D) Western blotting was used to detect the expression of PPAR γ /NF- κ B signaling pathway-related proteins. *** P <0.001 vs. Control; ** P <0.01 and *** P <0.001 vs. CSE. FX, fucoxanthin; PPAR γ , peroxisome proliferator-activated receptor γ ; STITCH, search tool for interactions of chemicals RT-qPCR, reverse transcription-quantitative polymerase chain reaction; CSE, cigarette smoke extract; p-, phosphorylated.

could effectively diminish ROS secretion and protect against oxidative stress and inflammation in bronchoalveolar lavage fluid (31). Another study suggested that FX could attenuate LPS-induced ALI via suppressing RhoA activation together with the NF- κ B pathway (32). However, the therapeutic effect of FX on COPD and its underlying mechanism have not been previously reported. The results of the present study demonstrated that FX significantly inhibited CSE-induced BEAS-2B cell inflammation and oxidative damage, thus supporting its effect on improving COPD.

Subsequently, the mechanism underlying the effect of FX on improving COPD was investigated. Analysis in the STITCH database predicted that PPAR γ could be a target of FX. Furthermore, the three-dimensional structure of PPAR γ was obtained from the PDB database. Autodock (version 4.2) database was used for molecular docking. A previous study on type 2 diabetic mice revealed that FX could distinctly increase PPAR γ expression in adipose tissue, thus improving the metabolism of sugar and fat (33). Herein, FX promoted the expression of PPAR γ and downregulated p-NF- κ B p65. It

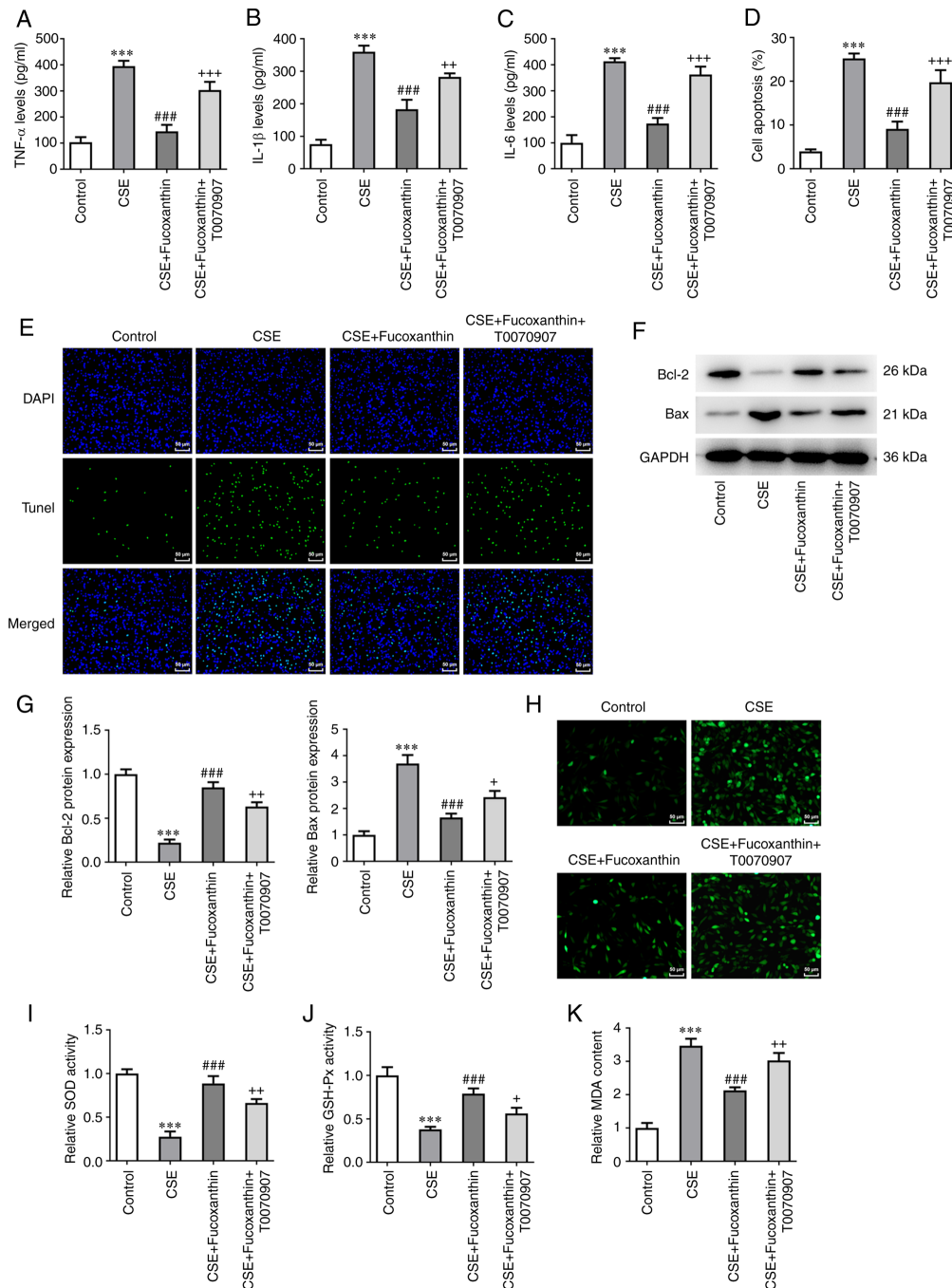


Figure 5. Pretreatment with the PPAR γ inhibitor, T0070907, reverses the protective effects of FX on CSE-induced BEAS-2B cells. Contents of (A) TNF- α , (B) IL-1 β and (C) IL-6 were examined using ELISA. (D and E) A TUNEL assay was used to determine the apoptotic rate of cells. (F and G) Western blotting was used to examine Bcl-2 and Bax expression. (H) DCFH-DA was used to assess ROS activity. Contents of (I) SOD, (J) GSH-Px and (K) MDA were examined using relative kits. ***P<0.001 vs. Control; ###P<0.001 vs. CSE; +P<0.05, ++P<0.01 and +++P<0.001 vs. CSE + Fucoxanthin. PPAR γ , peroxisome proliferator-activated receptor γ ; FX, fucoxanthin; CSE, cigarette smoke extract; TNF- α , tumor necrosis factor- α ; IL-, interleukin; ROS, reactive oxygen species; SOD, superoxide dismutase; GSH-Px, glutathione peroxidase; MDA, malondialdehyde.

was therefore hypothesized that PPAR γ may be a promising target in terms of pathophysiology and pharmacology for improving COPD. PPAR γ activation could possibly result in NF- κ B-dependent, GSE-induced and chemokine-mediated regulation of inflammatory responses (16). The expression levels of PPAR γ were reduced in primary human bronchial cells of patients with COPD compared with those in healthy smokers (34). Additionally, another study demonstrated that CSE-induced airway remodeling could be significantly

improved via activating the PPAR γ /TGF- β 1/Smad signaling pathway (35). Curcumin suppressed cigarette-induced inflammation via modulating the PPAR γ /NF- κ B signaling pathway, while PPAR γ inhibitor T0070907 inhibited this protective effect (36). Furthermore, a previous study revealed that PPAR γ inhibitor T0070907 downregulated the tight junction barrier function of human nasal epithelial cells through the PKC signaling pathway (37). FX was also demonstrated to downregulate the expression of PPAR γ

and inhibit adipogenesis in adipocytes, thereby exerting an anti-obesity effect (38). Therefore, it was hypothesized that FX may serve an important regulatory role in improving COPD via regulating the PPAR γ /NF- κ B signaling pathway. Herein, the protective effects of FX on CSE-induced cells were reversed following cell treatment with the PPAR γ inhibitor, T0070907.

FX was revealed to inhibit the inflammatory response by suppressing the activation of NF- κ B and MAPKs in lipopolysaccharide-induced RAW 264.7 macrophages (39). FX was also demonstrated to have anti-inflammatory activity in high-fat diet-induced obesity in mice and an antioxidant function in PC12 cells (40). FX suppressed lipid accumulation and ROS production during differentiation in 3T3-L1 adipocytes (41). FX and its metabolite, fucoxanthinol, suppressed adipocyte differentiation in 3T3-L1 cells (42). However, the regulation of FX on PPAR γ was not involved, and the regulation of FX on PPAR γ in COPD has not been reported to date, to the best of our knowledge, which is also the novelty of the present study.

The present study has certain limitations. Conclusions were drawn from cell experiments only, and have yet to be verified in animal experiments or clinical samples. *In vivo* experiments will be performed in future studies. In the present study, whether PPAR γ protein is a post-transcriptional regulator or stable protein was not determined, and to establish this, further experiments are required in the future. Moreover, the experiments were only carried out in one cell line, BEAS-2B cells, which is also a limitation of the present study.

In conclusion, the present study indicated that FX ameliorated oxidative damage and inflammation in CSE-induced human bronchial epithelial cells in patients with COPD via modulating the PPAR γ /NF- κ B signaling pathway.

Acknowledgements

Not applicable.

Funding

No funding was received.

Availability of data and materials

The datasets used and/or analyzed during the current study are available from the corresponding author on reasonable request.

Authors' contributions

SC and LZ conceived and designed the study. SC, JL and LZ performed the experiments. JL and LZ were major contributors to writing the manuscript. SC and LZ collected the clinical data and analyzed the data. All authors have read and approved the final manuscript. SC, LZ and JL confirm the authenticity of all the raw data.

Ethics approval and consent to participate

Not applicable.

Patient consent for publication

Not applicable.

Competing interests

The authors declare that they have no competing interests.

References

- Rabe KF and Watz H: Chronic obstructive pulmonary disease. *Lancet* 389: 1931-1940, 2017.
- Labaki WW and Rosenberg SR: Chronic obstructive pulmonary disease. *Ann Intern Med* 173: ITC17-ITC32, 2020.
- Vogelmeier CF, Criner GJ, Martinez FJ, Anzueto A, Barnes PJ, Bourbeau J, Celli BR, Chen R, Decramer M, Fabbri LM, *et al*: Global strategy for the diagnosis, management, and prevention of chronic obstructive lung disease 2017 report. GOLD executive summary. *Am J Respir Crit Care Med* 195: 557-582, 2017.
- Brandsma CA, Van den Berge M, Hackett TL, Brusselle G and Timens W: Recent advances in chronic obstructive pulmonary disease pathogenesis: From disease mechanisms to precision medicine. *J Pathol* 250: 624-635, 2020.
- Tashkin DP: Smoking cessation in chronic obstructive pulmonary disease. *Semin Respir Crit Care Med* 36: 491-507, 2015.
- Bae M, Kim MB, Park YK and Lee JY: Health benefits of fucoxanthin in the prevention of chronic diseases. *Biochim Biophys Acta Mol Cell Biol Lipids* 1865: 158618, 2020.
- Liu M, Li W, Chen Y, Wan X and Wang J: Fucoxanthin: A promising compound for human inflammation-related diseases. *Life Sci* 255: 117850, 2020.
- Gammone MA and D'Orazio N: Anti-obesity activity of the marine carotenoid fucoxanthin. *Mar Drugs* 13: 2196-2214, 2015.
- Meresse S, Fodil M, Fleury F and Chenais B: Fucoxanthin, a marine-derived carotenoid from brown seaweeds and microalgae: A promising bioactive compound for cancer therapy. *Int J Mol Sci* 21: 9273, 2020.
- Li X, Huang R, Liu K, Li M, Luo H, Cui L, Huang L and Luo L: Fucoxanthin attenuates LPS-induced acute lung injury via inhibition of the TLR4/MyD88 signaling axis. *Aging (Albany NY)* 13: 2655-2667, 2020.
- Ma SY, Park WS, Lee DS, Choi G, Yim MJ, Lee JM, Jung WK, Park SG, Seo SK, Park SJ, *et al*: Fucoxanthin inhibits profibrotic protein expression in vitro and attenuates bleomycin-induced lung fibrosis in vivo. *Eur J Pharmacol* 811: 199-207, 2017.
- Wu SJ, Liou CJ, Chen YL, Cheng SC and Huang WC: Fucoxanthin ameliorates oxidative stress and airway inflammation in tracheal epithelial cells and asthmatic mice. *Cells* 10: 1311, 2021.
- Mei C, Zhou S, Zhu L, Ming J, Zeng F and Xu R: Antitumor effects of laminaria extract fucoxanthin on lung cancer. *Mar Drugs* 15: 39, 2017.
- Feng H, Yin Y, Zheng R and Kang J: Rosiglitazone ameliorated airway inflammation induced by cigarette smoke via inhibiting the M1 macrophage polarization by activating PPAR γ and RXR α . *Int Immunopharmacol* 97: 107809, 2021.
- Qiu JF, Ma N, He ZY, Zhong XN, Zhang JQ, Bai J, Deng JM, Tang XJ, Luo ZL, Huang M, *et al*: Erythromycin inhibits cigarette smoke-induced inflammation through regulating the PPAR γ /NF- κ B signaling pathway in macrophages. *Int Immunopharmacol* 96: 107775, 2021.
- Solleti SK, Simon DM, Srisuma S, Arikian MC, Bhattacharya S, Rangasamy T, Bijli KM, Rahman A, Crossno JT Jr, Shapiro ST and Mariani TJ: Airway epithelial cell PPAR γ modulates cigarette smoke-induced chemokine expression and emphysema susceptibility in mice. *Am J Physiol Lung Cell Mol Physiol* 309: L293-L304, 2015.
- Kang SI, Ko HC, Shin HS, Kim HM, Hong YS, Lee NH and Kim SJ: Fucoxanthin exerts differing effects on 3T3-L1 cells according to differentiation stage and inhibits glucose uptake in mature adipocytes. *Biochem Biophys Res Commun* 409: 769-774, 2011.
- Lee AH, Shin HY, Park JH, Koo SY, Kim SM and Yang SH: Fucoxanthin from microalgae *Phaeodactylum tricornutum* inhibits pro-inflammatory cytokines by regulating both NF- κ B and NLRP3 inflammasome activation. *Sci Rep* 11: 543, 2021.

19. Dang X, He B, Ning Q, Liu Y, Guo J, Niu G and Chen M: Alantolactone suppresses inflammation, apoptosis and oxidative stress in cigarette smoke-induced human bronchial epithelial cells through activation of Nrf2/HO-1 and inhibition of the NF- κ B pathways. *Respir Res* 21: 95, 2020.
20. O'Boyle NM, Banck M, James CA, Morley C, Vandermeersch T and Hutchison GR: Open babel: An open chemical toolbox. *J Cheminform* 3: 33, 2011.
21. Berman H, Henrick K and Nakamura H: Announcing the worldwide protein data bank. *Nat Struct Biol* 10: 980, 2003.
22. Morris GM, Huey R, Lindstrom W, Sanner MF, Belew RK, Goodsell DS and Olson AJ: AutoDock4 and AutoDockTools4: Automated docking with selective receptor flexibility. *J Comput Chem* 30: 2785-2791, 2009.
23. Livak KJ and Schmittgen TD: Analysis of relative gene expression data using real-time quantitative PCR and the 2(-Delta Delta C(T)) method. *Methods* 25: 402-408, 2001.
24. Chen L, Yuan X, Zou L, Peng J and Hu X: Effects of 1,25-Dihydroxyvitamin D3 on the prevention of chronic obstructive pulmonary disease (COPD) in rats exposed to air pollutant particles less than 2.5 micrometers in diameter (PM2.5). *Med Sci Monit* 24: 356-362, 2018.
25. Kohansal R, Martinez-Cambor P, Agusti A, Buist AS, Mannino DM and Soriano JB: The natural history of chronic airflow obstruction revisited: An analysis of the Framingham offspring cohort. *Am J Respir Crit Care Med* 180: 3-10, 2009.
26. Kankaanranta H, Harju T, Kilpelainen M, Mazur W, Lehto JT, Katajisto M, Peisa T, Meinander T and Lehtimäki L: Diagnosis and pharmacotherapy of stable chronic obstructive pulmonary disease: The finnish guidelines. *Basic Clin Pharmacol Toxicol* 116: 291-307, 2015.
27. Vestbo J, Hurd SS, Agusti AG, Jones PW, Vogelmeier C, Anzueto A, Barnes PJ, Fabbri LM, Martinez FJ, Nishimura M, *et al*: Global strategy for the diagnosis, management, and prevention of chronic obstructive pulmonary disease: GOLD executive summary. *Am J Respir Crit Care Med* 187: 347-365, 2013.
28. Lopez-Campos JL, Tan W and Soriano JB: Global burden of COPD. *Respirology* 21: 14-23, 2016.
29. Barnes PJ: Oxidative stress-based therapeutics in COPD. *Redox Biol* 33: 101544, 2020.
30. Chen W, Zhang H and Liu Y: Anti-inflammatory and apoptotic signaling effect of fucoxanthin on benzo(A)pyrene-induced lung cancer in mice. *J Environ Pathol Toxicol Oncol* 38: 239-251, 2019.
31. Yang X, Guo G, Dang M, Yan L, Kang X, Jia K and Ren H: Assessment of the therapeutic effects of fucoxanthin by attenuating inflammation in ovalbumin-induced asthma in an experimental animal model. *J Environ Pathol Toxicol Oncol* 38: 229-238, 2019.
32. Lee CY, Chen SP, Huang-Liu R, Gau SY, Li YC, Chen CJ, Chen WY, Wu CN and Kuan YH: Fucoxanthin decreases lipopolysaccharide-induced acute lung injury through the inhibition of RhoA activation and the NF- κ B pathway. *Environ Toxicol* 37: 2214-2222, 2022.
33. Lin HV, Tsou YC, Chen YT, Lu WJ and Hwang PA: Effects of low-molecular-weight fucoidan and high stability fucoxanthin on glucose homeostasis, lipid metabolism, and liver function in a mouse model of type II diabetes. *Mar Drugs* 15: 113, 2017.
34. Kwak N, Lee KH, Woo J, Kim J, Lee CH and Yoo CG: Synergistic cycles of protease activity and inflammation via PPAR γ degradation in chronic obstructive pulmonary disease. *Exp Mol Med* 53: 947-955, 2021.
35. Pan K, Lu J and Song Y: Artesunate ameliorates cigarette smoke-induced airway remodelling via PPAR- γ /TGF- β 1/Smad2/3 signalling pathway. *Respir Res* 22: 91, 2021.
36. Li Q, Sun J, Mohammadtursun N, Wu J, Dong J and Li L: Curcumin inhibits cigarette smoke-induced inflammation via modulating the PPAR γ -NF- κ B signaling pathway. *Food Funct* 10: 7983-7994, 2019.
37. Ogasawara N, Kojima T, Go M, Ohkuni T, Koizumi J, Kamekura R, Masaki T, Murata M, Tanaka S, Fuchimoto J, *et al*: PPARgamma agonists upregulate the barrier function of tight junctions via a PKC pathway in human nasal epithelial cells. *Pharmacol Res* 61: 489-498, 2010.
38. Koo SY, Hwang JH, Yang SH, Um JI, Hong KW, Kang K, Pan CH, Hwang KT and Kim SM: Anti-obesity effect of standardized extract of microalga *phaeodactylum tricornutum* containing fucoxanthin. *Mar Drugs* 17: 311, 2019.
39. Kim KN, Heo SJ, Yoon WJ, Kang SM, Ahn G, Yi TH and Jeon YJ: Fucoxanthin inhibits the inflammatory response by suppressing the activation of NF- κ B and MAPKs in lipopolysaccharide-induced RAW 264.7 macrophages. *Eur J Pharmacol* 649: 369-375, 2010.
40. Tan CP and Hou YH: First evidence for the anti-inflammatory activity of fucoxanthin in high-fat-diet-induced obesity in mice and the antioxidant functions in PC12 cells. *Inflammation* 37: 443-450, 2014.
41. Seo MJ, Seo YJ, Pan CH, Lee OH, Kim KJ and Lee BY: Fucoxanthin suppresses lipid accumulation and ROS production during differentiation in 3T3-L1 adipocytes. *Phytother Res* 30: 1802-1808, 2016.
42. Maeda H, Hosokawa M, Sashima T, Takahashi N, Kawada T and Miyashita K: Fucoxanthin and its metabolite, fucoxanthinol, suppress adipocyte differentiation in 3T3-L1 cells. *Int J Mol Med* 18: 147-152, 2006.



This work is licensed under a Creative Commons Attribution-NonCommercial-NoDerivatives 4.0 International (CC BY-NC-ND 4.0) License.